

A 3-D simulation with virtual stereo rig for centrifugal fertilizer spreading

Bilal Hijazi^{1&2}, Jürgen Vangeyte², Frédéric. Cointault^{1*}, Michel Paindavoine⁴, Jan Pieters³

¹AgroSup Dijon – UP GAP – 26, Bd Dr Petitjean – BP 87999 – 21079 Dijon cedex – France

²Institute for Agricultural and Fisheries Research (ILVO) - Technology and Food Science – Agricultural Engineering – Burg. Van Gansberghelaan 115 – 9820 Merelbeke – Belgium

³Department of Biosystems Engineering – Faculty of Bioscience Engineering - Ghent University – Coupure Links 653 - 9000 Gent - Belgium

⁴LEAD – UMR CNRS 5022 – University of Burgundy – Pôle AAFE – BP 26513 – 21065 Dijon cedex – France

**Corresponding author: f.cointault@agrosupdijon.fr*

Abstract

Stereovision can be used to characterize of the fertilizer centrifugal spreading process and to control the spreading fertilizer distribution pattern on the ground reference. Fertilizer grains, however, resemble each other and the grain images contain little information on texture. Therefore, the accuracy of stereo matching algorithms in literature cannot be used as a reference for stereo images of fertilizer grains.

In order to evaluate stereo matching algorithms applied to images of grains a generator of synthetic stereo particle images is presented in this paper. The particle stereo image generator consists of two main parts: the particle 3D position generator and the virtual stereo rig. The particle 3D position generator uses a simple ballistic flight model and the disc characteristics to simulate the ejection and the displacement of grains. The virtual stereo rig simulates the stereo acquisition system and generates stereo images, a disparity map and an occlusion map. The results are satisfying and present an accurate reference to evaluate stereo particles matching algorithms.

Keywords: fertilizer centrifugal spreader, stereovision, image processing.

1. Introduction

With respect to centrifugal fertilizer spreading, many factors, such as construction and calibration of the machinery, particle types and properties, field conditions, etc. influence the distribution pattern in the field (Cointault et al., 2008; Hijazi et al., 2010b; Hijazi et al., 2011; Van Liedekerke et al., 2009). Maladjusted centrifugal spreaders create heterogeneous distributions with economical and environmental consequences.

In previous work (Hijazi et al., 2010a; Hijazi et al., 2010c), the feasibility of stereovision to characterize the fertilizer centrifugal spreading process and to control the spreading fertilizer distribution pattern on the ground was already demonstrated. Imaging systems, specifically stereo rig, are lately being more widely used in several domains (Ayache, 1989; Durdle et al., 1998; Hori, 2004; Michoud, 2009). Several procedural steps are necessary in stereovision: camera calibration, image acquisition, image rectification, image matching and depth determination.

The major task in stereo computing is image matching. Image matching is the determination of the correspondence between pixels of the right and left images. If matching is accurate, depth calculation will be accurate as well. However, image matching is difficult. Its accuracy depends on several factors such as image resolution, noises, texture, etc. Fertilizer grains all look alike and their images contain little information on their texture. As a result the accuracy of stereo matching algorithm in literature cannot be used as a reference for a stereo images of fertilizer grain.

In order to evaluate stereo matching algorithms applied to grain images in this paper a generator of synthetic stereo particle images is presented.

2. Fertilizer grain centrifugal spreading process simulator

The grains are assumed to be spherical. The 3D particle simulator generates the 3D coordinates and the sizes of the particles. The output of the simulator can depend on the application. Since our application is centrifugal spreading particle, positions are generated with modeling of the process in question.

3. Virtual stereo rig

The pinhole model (Hartley&Zisserman, 2000) was used to simplify the camera system. Hence, two characteristics of cameras, pixel dimension and sensor resolution, and the focal length are needed to simulate a camera. The optical axes of both cameras of the stereo system were supposed to be parallel. Consequently, the translation between the cameras is known.

The output of the virtual stereo rig are the stereo images, the disparity map and the occlusion map. The procedure for the creation of both the right and the left images is as follows, starting with the left image.

First, the line L are drawn from the left optical center (C_L) through the center of each pixel p_i . When the line L crosses a sphere or particle the grey level of the pixel p_i (FIGURE1) changes. The value of the grey level is determined by a Gaussian distribution function. The maximum of the Gaussian function corresponds to the center of the sphere. The final value that is assigned to the pixel is proportional to the distance between the sphere and the optical center. This results in the simulated left image.

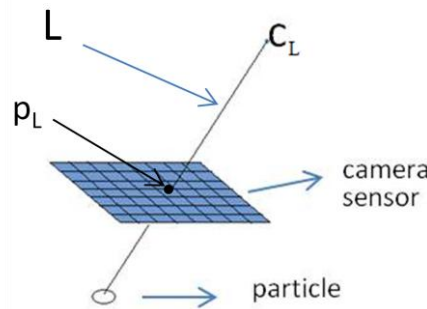


FIGURE1: Illustration of the virtual image acquisition process. C is the optical center

Next, the right image is simulated. The intersections between L and the spheres or particles are connected to the right optical center C_R by a line L_R . If L_R crosses another sphere in the direction of C_R , the pixel in the occlusion map corresponding to p_i is put to one. The occlusion map is an image matrix of the points in the field of view that can only be seen in the left image. In the other case, a grey level is assigned to the pixel p_r on the intersection between L_R and the right image plane. In addition, the disparity map pixel that corresponds to p_i is put to $d=x_i-x_r$ (x_i and x_r are the abscissa of p_i and p_r , respectively) in the right image. The centers of pixels that are not assigned a grey level are connected to optical center with a line R . If line R crosses a sphere then the grey level, determined by the Gaussian function and the distance are assigned to the pixel. The method is summarized schematically in figure 2.

4. Performing the simulations

4.1 Virtual stereo rig characteristics

The first step was to define the cameras' characteristics. The tests were performed with virtual stereo system characteristics equivalent to the real set-up used during the measurement (Cointault et al., 2003; Villette et al., 2007). The sensor resolution and size were chosen in such a way that the conversions [pixels/mm] were the same in the simulation as for the real set-up. The virtual stereo system characteristics are:

- Focal length: 28 mm

- Pixel size: 12 μ m x12 μ m
- Sensor size: 2000x2000 pixels
- Camera distance from the work plane: 2 m
- Baseline (horizontal translation between cameras): 0.15 m

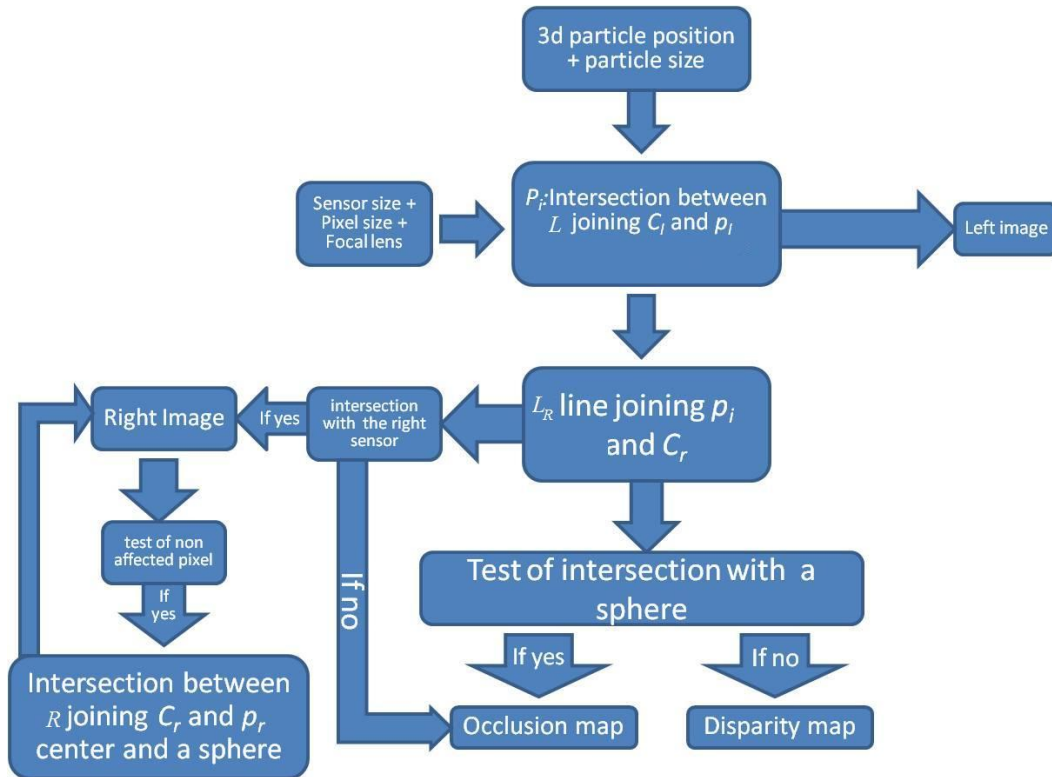


FIGURE. 2: Graph illustrating the algorithm used to create stereo images, the disparity map and the occlusion map.. C_l and C_r are respectively left and right optical center. p_l and p_r are respectively left and right sensor pixel center. L is a line passing by C_l and L_R & R are lines passing by C_r

4.2 Ballistic model

The second step was to define a model that simulates the distribution of the grains. Therefore a simple ballistic flight model generated the grain coordinates in space. Ejection speed and vertical and horizontal ejection angles were determined based on values obtained from measurements with our experimental test set-up. The input parameters were:

- The initial positions of the grain at ejection;
- The ejection speed (V);
- The vertical and horizontal ejection angles (θ_v and θ_h)
- The initial positions of the grains determined by the mean grain size and two characteristics of the centrifugal spreader:
 - The rotation speed of the spreader disk (Ω)
 - The vane length (L_{vane})

An ejected grain of mass m and velocity v is subjected to two forces, gravity and air resistance (Fig .3). The air resistance is assumed to be in the opposite direction of the grain motion $\vec{F}_{air} = -k \cdot v \cdot \vec{v}$. The ballistic model did not take into account the spinning of the grains.

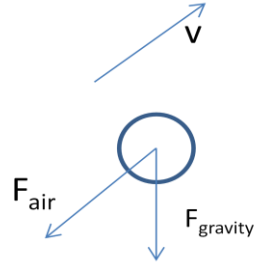


FIGURE 3: Forces applied to a grain: v is the speed of the grain F_{air} is the air resistance and F_{gravity} is the gravity force.

Applying Newton's second law the motion equations were established. Thereafter, The algorithm of 3D grain coordinates generation is described in figure 4.

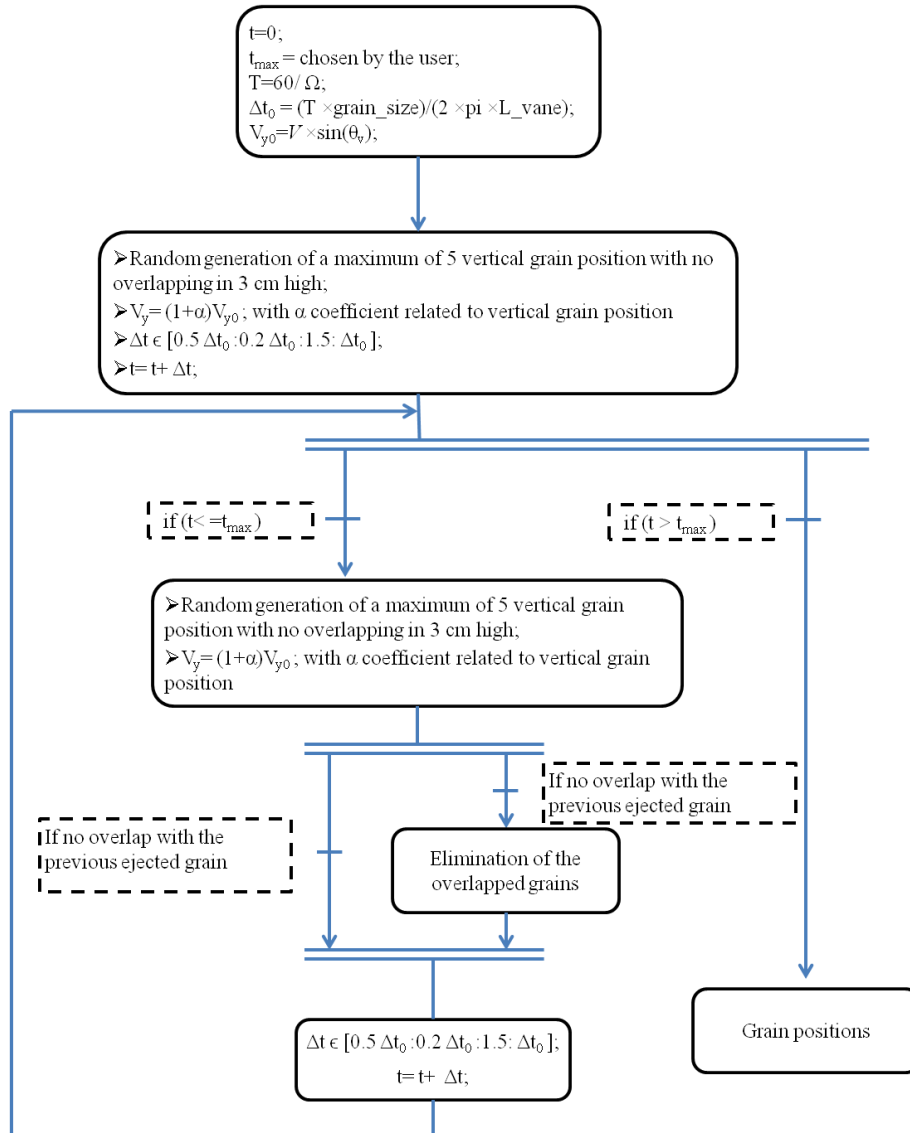


FIGURE 4: algorithm of 3D grain coordinates generation; Ω is the rotation speed of the disk, $grain_size$ is the size of the grain, L_vane is the length of the vane, θ_v and θ_h are the vertical and horizontal ejection angles, Δt_0 is the mean delay between the ejection of two grains and V_{y0} is the minimum vertical ejection speed.

4.3 Simulation results

The simulations were performed using parameters determined from a real centrifugal spreading process. FIGURE 5 shows the calculated coordinates for the following parameters:

- rotation speed of the spreader disk :800 tr/min
- vane length: 300 mm
- minimum vertical ejection angle: 6°
- horizontal ejection angle: 50°
- velocity $V = 40m.s^{-1}$

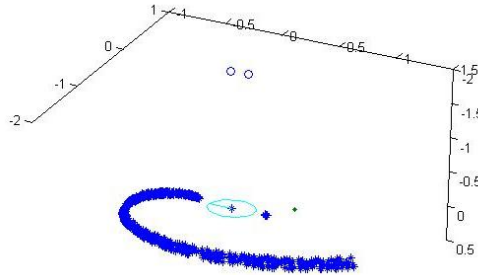


FIGURE 5 The two small circle on the top of the image represent the cameras, the circle at the position (0,0,0) represent the disk and the arc shaped cloud of points represent the centers of particles .

Using the generated positions, the stereo synthetic images (

FIGURE 6) were created via the virtual stereo rig.

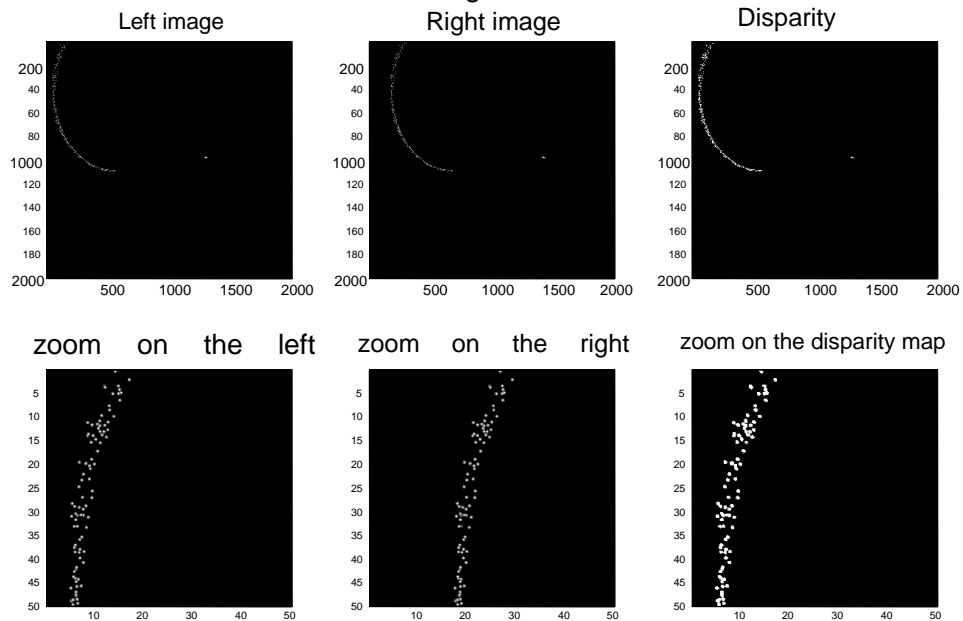


FIGURE 6: resulting images of a fertilizer grain centrifugal spreading simulation: (a) left stereo image and (b) right stereo image. (c) disparity map and (d) occlusion map.

Conclusion

We presented in this paper a particle stereo image generator. The outputs of the generator are the stereo images, disparity map and the occlusion map which can be used to evaluate the stereo matching algorithms used on stereo images of particles.

In future work the generator will be extended to generate images of particles in motion in order to evaluate 3D motion estimation methods applied on particles motion.

References

Ayache, N. (1989). *Vision Stéréoscopique et perception multisensorielle: applications à la robotique mobile*. InterEditions, Paris.

Cointault, F., Sarrazin, P., & Paindavoine, M. (2003). Measurement of the motion of fertilizer particles leaving a centrifugal spreader using a fast imaging system. *Precision Agriculture* **4**, 279-295.

Cointault, F., Vangeyte, J., Dubois, J., Baert, J., & Clerc, C. (2008). New high speed imaging system for fertilizer granule characterisation at the ejection. *In International Conference on Agricultural Engineering & Industry Exhibition*, pp. OP-1555. European Society of Agricultural Engineers (AgEng).

Durdle, N. G., Thayyoor, J., & Raso, V. J. (1998). An improved structured light technique for surface reconstruction of the human trunk. *In Electrical and Computer Engineering, 1998. IEEE Canadian Conference on*, Vol. 2, pp. 874-877 vol.2.

Hartley, R., & Zisserman, A. (2000). *Multiple view geometry in computer vision*. Cambridge: Cambridge Univ Press.

Hijazi, B., Baert, J., Cointault, F., Dubois, J., Paindavoine, M., Pieters, J., & Vangeyte, J. (2010a). A device for extracting 3D information of fertilizer trajectories. *In the XVIth World Congress of the International Commission of Agricultural Engineering (CIGR)*, Quebec city, Canada.

Hijazi, B., Cointault, F., Dubois, J., Coudert, S., Vangeyte, J., Pieters, J., & Paindavoine, M. (2010b). Multi-phase cross-correlation method for motion estimation of fertiliser granules during centrifugal spreading. *Precision Agriculture* **11**, 684-702.

Hijazi, B., Cointault, F., Vangeyte, J., Dubois, J., Paindavoine, M., & Pieters, J. (2010c). A 3-D stereovision system for fertilizer granule characterization. *In AgEng Cemagref, Clermont-Ferrand, France*.

Hijazi, B., Vangeyte, J., Cointault, F., Dubois, J., Coudert, S., Paindavoine, M., & Pieters, J. (2011). Two-step cross correlation-based algorithm for motion estimation applied to fertilizer granules motion during centrifugal spreading. *Optical Engineering* **50**, 067002.

Hori, T., Sakakibara, J. (2004). High Speed Scanning Stereoscopic PIV for 3D Vorticity Measurement in Liquids. *Measurement Science and Technology* **15 No.6**, 1067-1078. .

Michoud, B. (2009). *Reconstruction 3D à partir de séquences vidéo pour l'acquisition du mouvement de personnages en temps réel et sans marqueur*, Université Claude Bernard Lyon 1.

Van Liedekerke, P., Tijssens, E., Dintwa, E., Rioual, F., Vangeyte, J., & Ramon, H. (2009). DEM simulations of the particle flow on a centrifugal fertilizer spreader. *Powder Technology* **190**, 348-360.

Villette, S., Cointault, F., Zwaenepoel, P., Chopinet, B., & Paindavoine, M. (2007). Velocity measurement using motion blurred images to improve the quality of fertiliser spreading in agriculture. *In The Eight International Conference on Quality Control by Artificial Vision (D. Fofi & F. Meriaudeau, eds.)*. Spie, Le Creusot, France.